RESEARCH ARTICLE   OPEN ACCESS

A Novel Feature Extraction Scheme for Medical X-Ray Images

[1]Prachi.G.Bhende, [2]Dr.A.N.Cheeran
Department of Electrical Engineering, VJTI, Mumbai, India
Department of Electrical Engineering, VJTI, Mumbai, India

ABSTRACT
X-ray images are gray scale images with almost the same textural characteristic. Conventional texture or color features cannot be used for appropriate categorization in medical x-ray image archives. This paper presents a novel combination of methods like GLCM, LBP and HOG for extracting distinctive invariant features from X-ray images belonging to IRMA (Image Retrieval in Medical applications) database that can be used to perform reliable matching between different views of an object or scene. GLCM represents the distributions of the intensities and the information about relative positions of neighboring pixels of an image. The LBP features are invariant to image scale and rotation, change in 3D viewpoint, addition of noise, and change in illumination A HOG feature vector represents local shape of an object, having edge information at plural cells. These features have been exploited in different algorithms for automatic classification of medical X-ray images. Excellent experimental results obtained in true problems of rotation invariance, particular rotation angle, demonstrate that good discrimination can be achieved with the occurrence statistics of simple rotation invariant local binary patterns.
Keywords: Gray level co-occurrence matrix (GLCM), Local Binary Pattern (LBP), Histogram of Oriented Gradients (HOG)

I. INTRODUCTION

Textures provide essential information for many image classification tasks. Much research has been done on texture classification during the last three decades, most traditional approaches include gray level co-occurrence matrices (GLCM), second-order statistic method, Gauss–Markov random field and local linear transform, which are restricted to the analysis of spatial relations between neighboring pixels in a small image region [1,2]. In various applications, to deal with the semantic gap trouble, texture features are employed. For example, it is used to explain organ's tissues in the medical imaging field. Thus, the majority of the research in the area of texture analysis is devoted to developing the inequitable capability of the features extracted from the image. Recently many local descriptors are proposed for object recognition and image retrieval. Local binary pattern (LBP), a non-parametric technique summarizing the local structures of an image efficiently, is one of the most used texture descriptors in image analysis. LBP was initially proposed by Timo Ojala for texture description and has been broadly exploited in numerous applications. The most important properties of LBP features are tolerance against the monotonic illumination changes and computational simplicity as well [3]. In recent years, LBP features have been extensively exploited for facial image analysis, together with face detection, face recognition; facial expression analysis, gender/age categorization and some other applications. In the meantime, different variations of the original LBP have been proposed for an improved performance. This work focuses on gray-scale and rotation invariant texture classification, which has been addressed by Chen and Kundu [4] and Wu and Wei [5]. Both studies approached gray-scale invariance by assuming that the gray-scale transformation is a linear function. This is a somewhat strong simplification, which may limit the usefulness of the proposed methods. Chen and Kundu realized gray-scale invariance by global normalization of the input image using histogram equalization. This is not a general solution however, as global histogram equalization cannot correct intra image (local) gray-scale variations [4]. Mikolajczyk *et al.* compared the performance of the several local descriptors and showed that the best matching results were obtained by the Scale Invariant Feature Transform (SIFT) descriptor [6]. Dalal *et al.* [7] proposed a human detection algorithm using histograms of oriented gradients (HOG) which are similar with the features used in the SIFT descriptor. HOG features are calculated by taking orientation histograms of edge intensity in a local region. They are designed by imitating the visual information processing in the brain and have robustness for local changes of appearances, and position. Dalal *et al.* extracted the HOG features from all locations of a dense grid from an image region and the combined features are classified by using linear SVM. They showed that the grids of HOG descriptors significantly outer-performed existing feature sets for human detection. Ke *et al.* applied Principal

Components Analysis (PCA) to reduce the dimensionality of the feature vectors and tested them in an image retrieval application [8]. There are also many other feature detection methods, as edge detection, corner detection, etc. which have their own advantages. As the x-ray images are characterized with contrast variation and non-uniform intensity background, weak signal-to-noise ratio, digitized x-ray projections noise, and high frequency noise, extracting desired features is quite challenging.

The work carried out in this paper focuses on deriving a set of unique feature vectors to support easy and fast medical X-Ray image classification using a combination of global texture and local features by applying GLCM, LBP, HOG techniques. In the next section, the proposed algorithms are discussed. Then the experimental results are described in section 3. The conclusion and the future works are given in section 4.

II. METHODOLOGY and RESULT ANALYSIS

Feature detection and matching are essential components of many computer vision applications. Texture is an important characteristics used in identifying regions of interest in an image [9]. Among the variety of techniques available for feature extraction the following methods based on local and global feature extraction process are applied to the X-ray Images belonging to IRMA database as they can deal with gray level variations problem efficiently.

2.1. Implementation of Grey Level Co-occurrence Matrices

Grey Level Co-occurrence Matrices (GLCM) is one of the well-known texture extraction techniques which measures second order texture characteristics. One of the simplest approaches for describing texture is to use statistical moments of the intensity histogram of an image or region [10, 11]. Using only histograms in calculation will result in measures of texture that carry only information about distribution of intensities, but not about the relative position of pixels with respect to each other in that texture. Using a statistical approach such as co-occurrence matrix will help to provide valuable information about the relative position of the neighbouring pixels in an image.

The GLCM of an $N \times N$ image, containing pixels with gray levels 0, 1, 2…., $G-1$ is a matrix $P(i, j)$, where each element of the matrix represents the probability of joint occurrence of intensity levels i and j at a certain distance and an angle θ, is calculated. The four occurrence matrixes of GLCM

are obtained from four different directions ($\theta° \{0°, 90°, 45°,$ and $135°\}$) at global level.

Co-occurrence: Given an image I, of size $N \times N$, the co-occurrence, matrix P can be defined as

$$P(i,j) = \sum_{x=1}^{N} \sum_{y=1}^{N} \begin{cases} 1, & if\ I(x,y) = i\ and\ I(x + \Delta x, y + \Delta y) = j \\ 0, & otherwise \end{cases}$$

(1)

Here, the offset (Δx, Δy), is specifying the distance between the pixel-of-interest and its neighbour. Note that the offset (Δx, Δy) parameterization makes the co-occurrence matrix sensitive to rotation. Choosing an offset vector, such that the rotation of the image is not equal to 180 degrees, will result in a different co-occurrence matrix for the same (rotated) image. This can be avoided by forming the co-occurrence matrix using a set of offsets sweeping through 180 degrees at the same distance parameter D to achieve a degree of rotational invariance (i.e., [0 D] for 0° : **P** horizontal, [-D D] for 45° : **P** right diagonal, [-D 0] for 90° : **P** vertical, and [-D -D] for 135° : **P** left diagonal).These measures are arrays termed angular nearest neighbour spatial dependence matrices, which considers nearest resolution cells in particular direction.
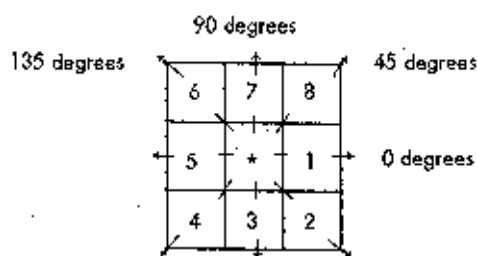
Figure2.1.Resolution cells1and 5 are 0°(horizontal) nearest neighbors to center pixel(resolution cell) *;resolution cells 2 and 6 are 135° nearest neighbors; resolution cells 4 and 8 are 45° nearest neighbors; resolution cells 3 and 7 are 90° nearest neighbors to *.

Figure 2.2 illustrates the details of the process to generate the four co-occurrence matrices using $Ng = 5$ levels for the offsets ʃ[0 1], [-1 1], [-1 0], [-1 -1]ʃ that are defined as one neighboring pixel in the possible four directions. We can see that two neighboring pixels (2, 1) of the input image is reflected in P_H concurrence matrix as 3, because there are 3 occurrences of the pixel intensity value 2 and pixel intensity value 1 adjacent to each other in the input image. The neighboring pixels (1, 2) will occur again 3 times in P_H, which makes these matrices symmetric. In the same manner, the other three matrices P_V, P_{LD}, P_{RD} are calculated.
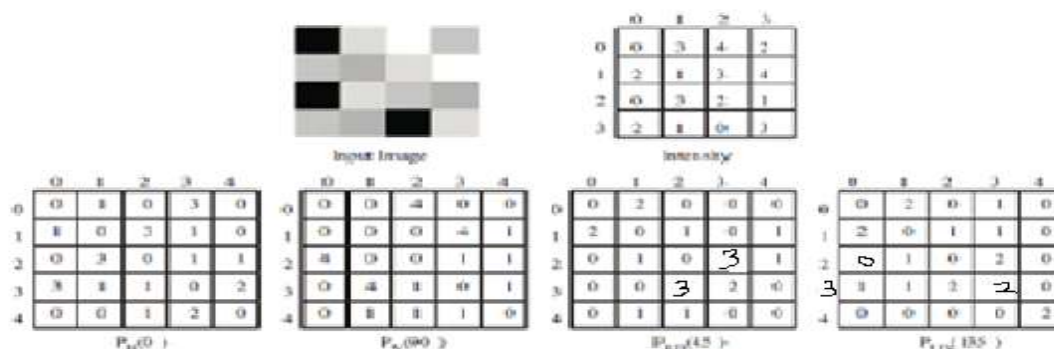
Figure 2.2 Implementation of GLCM for four different offsets [11]

The four matrices can be used separately for classification, and then the final decision can be formed by fusing the four decisions. As these matrices are symmetric, it is more convenient to use the upper or lower diagonal matrix coefficients in forming the vectors. So, instead of having a vector length of $Ng \times Ng$, the vector size is reduced to $(Ng \times Ng + Ng)/2$ which helps to speed up the process without affecting the recognition performance. Applying this technique to a gray scale X-ray image (P_{ij}) of hand had given the texture context information adequately, as a gray tone spatial dependence matrix which is function of the angular relationship between the neighbouring resolution cells as well as a function of distance between them.

2.2. Implementation of Local Binary Pattern

In this method a gray scale and rotation invariant texture operator based on local binary patterns (LBP) proposed by Ojala [3] is applied for the medical x-ray images from IRMA database. Starting from the joint distribution of gray values of a circularly symmetric neighbor set of eight pixels in a 3×3 neighborhood, we derive an operator that is by definition invariant against any monotonic transformation of the gray scale. Rotation invariance is achieved by recognizing that this gray scale invariant operator incorporates a fixed set of rotation invariant patterns.

I: Gray Scale and Rotation Invariant Local Binary Patterns

We start the derivation of gray scale and rotation invariant texture operator by defining texture T in a local 3×3 neighborhood of a monochrome texture image as the joint distribution of the gray levels of the nine image pixels:

$$T = P\,(g_0, g_1, g_2, g_3, g_4, g_5, g_6, g_7, g_8) \qquad (2)$$

where gi ($I = 0, 1, .., 8$), correspond to the gray values of the pixels in the 3×3 neighborhood according to the spatial layout illustrated in Fig. 2.2. The gray

values of diagonal pixels ($g2$, $g4$, $g6$, and $g8$) are determined by interpolation.
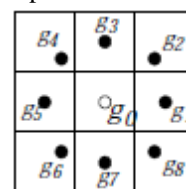
Figure2.3: The circularly symmetric neighbour set of eight pixels in a 3×3 neighborhood

II: Achieving Gray Scale Invariance

As the first step towards gray scale invariance we subtract, without losing information, the gray value of the centre pixel ($g0$) from the gray values of the eight surrounding pixels of the circularly symmetric neighborhood (gi, $I = 1,..., 8$) giving:

$$T = P\,(g_0, g_1 - g_0, g_2 - g_0, g_3 - g_0, g_4 - g_0, g_5 - g_0, g_6 - g_0, g_7 - g_0, g_8 - g_0) \qquad (3)$$

Next, assume that differences $gi - g0$ are independent of $g0$, which allows to factorize Eq. (3):

$$T \approx P\,(g_0)\,P(g_1 - g_0, g_2 - g_0, g_3 - g_0, g_4 - g_0, g_5 - g_0, g_6 - g_0, g_7 - g_0, g_8 - g_0) \qquad (4)$$

Signed differences $gi - g0$ are not affected by changes in mean luminance, hence the joint difference distribution is invariant against gray scale shifts. We achieve invariance with respect to the scaling of the gray scale by considering just the signs of the differences instead of their exact values:

$$T \approx p(s\,(g_1 - g_0), \; s(g_2 - g_0), \; s(g_3 - g_0), \; ......, \; s(g_8 - g_0))......... \qquad (5)$$

Where

$$s(x) = \begin{cases} 1, & x \geq 0 \\ 0, & x < 0 \end{cases} \qquad (6)$$

If eq. (5) is formulated slightly differently, an expression similar to the LBP (Local Binary Pattern) operator is obtained:

$$\text{LBP}_8 = \sum_{i=1}^{8} s(gi - g0)\,2^{i-1} \qquad (7)$$

The two differences between LBP$_8$ and the LBP operator are: 1) the pixels in the neighbor set are indexed so that they form a circular chain, and 2) the gray values of the diagonal pixels are determined by interpolation. Both modifications are necessary to obtain the circularly symmetric neighbor set, which allows for deriving a rotation invariant version of LBP$_8$. For notational reasons we augment LBP with subscript 8 to denote that the LBP$_8$ operator is determined from the 8 pixels in a 3×3 neighborhood [12].

III: Achieving Rotation Invariance

The LBP$_8$ operator produces 256 (2^8) different output values, corresponding to the 256 different binary patterns that can be formed by the eight pixels in the neighbor set. When the image is rotated, the gray values g_i will correspondingly move along the perimeter of the circle around g_0. Since we always assign g_1 to be the gray value of element (0, 1), to the right of g_0, rotating a particular binary pattern naturally results in a different LBP$_8$ value [13]. This does not apply to patterns 00000000$_2$ and 11111111$_2$

which remain constant at all rotation angles. To remove the effect of rotation, i.e. to assign a unique identifier to each rotation invariant local binary pattern we define:

$$LBP_8^{rI36} = \min\{ROR(\text{LBP8}, i)\} \quad i = 0,1,....,7\} \quad (8)$$

where *ROR (x, i)* performs a circular bit-wise right shift on the 8-bit number *x i* times. In terms of image pixels eq. (8) simply corresponds to rotating the neighbor set clockwise so many times that a maximal number of the most significant bits, starting from g_8 are 0. We observe that LBP_8^{rI36} can have 36 different values, corresponding to the 36 unique rotation invariant local binary patterns illustrated in Fig. 2.4, hence the superscript *ri36*. LBP$_8^{ri36}$ quantifies the occurrence statistics of these patterns corresponding to certain micro features in the image, hence the patterns can be considered as feature detectors. For example, pattern #0 detects bright spots, #8 dark spots and flat areas, and #4 edges. Hence, obtained the gray scale and rotation invariant operator LBP_8^{rI36} that was designated as LBPROT in [14].
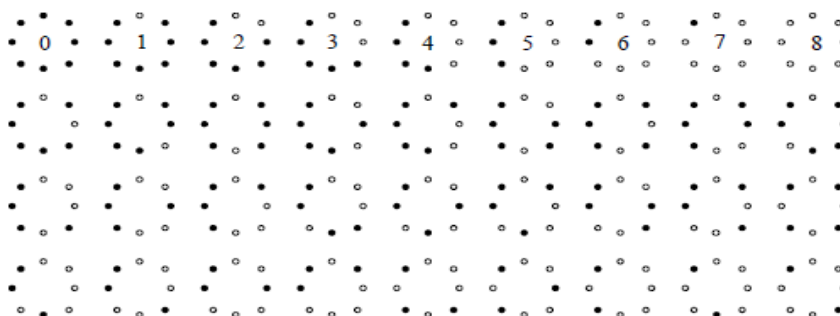
Figure 2.4 The 36 unique rotation invariant binary patterns that can occur in the eight pixel circularly symmetric neighbor set. Black and white circles correspond to bit values of 0 and 1 in the 8-bit output of the LBP$_8$ operator. The first row contains the nine 'uniform' patterns and the number inside them corresponds to their unique LBP$_8$^{riu2} values.

IV: Improved Rotation Invariance with 'Uniform' Patterns

However, practical experiments showed that LBP_8^{rI36} as such does not provide a very good discrimination. There are two reasons:

1) the performance of the 36 individual patterns in discrimination of rotated textures varies greatly: while some patterns sustain rotation quite well, other patterns do not and only confuse the analysis. Consequently, using all 36 patterns leads to a suboptimal result (as addressed above).

2) crude quantization of the angular space at 45° intervals

The varying performance of individual patterns attributes to the spatial structure of the patterns. To quantify this we define an uniformity measure U ('pattern'), which corresponds to the number of spatial transitions (bitwise 0/1 changes) in the pattern [15]. The larger the uniformity value U of a pattern,

the larger number of spatial transitions occurs in the pattern, the more likely the pattern is to change to a different pattern upon rotation in digital domain. Based on this argument we designate patterns that have U value of at most 2 as 'uniform' and propose the following operator for gray scale and rotation invariant texture description instead of LBP_8^{rI36}:

$$LBP_8^{riu2} = \begin{cases} \sum_{i=1}^{8} s(gi - g0) & \text{if } U(\text{LBP}_8) \leq 2 \\ 9 & otherwise \end{cases}$$
(9)

Equation (9) corresponds to giving a unique label to the nine uniform patterns illustrated in the first row of Fig. 2.3 (label corresponds to the number of '1' bits in the pattern), the 27 other patterns being grouped under the miscellaneous label (9). Superscript *riu2* corresponds to the use of *r*otation *in*variant *u*niform patterns that have U value of at most *2*.

The selection of uniform patterns with the simultaneous compression of non-uniform patterns is

also supported by the fact that the former tend to dominate in deterministic texture.

V: Improved Angular Resolution with a 16 pixel neighborhood

It was noted earlier that the rotation invariance of LBP_8^{riu2} is hampered by the crude 45° quantization of the angular space provided by the neighbor set of eight pixels. To address this a modification was presented, where the angular space is quantized at a finer resolution of 22.5° intervals. This is accomplished with the circularly symmetric neighbor set of 16 pixels illustrated in Fig.2.5. Again, the gray values of neighbors which do not fall exactly in the centre of pixels are estimated by interpolation. Note that increase the size of the local neighborhood to 5 × 5 pixels, as the eight added neighbors would not provide too much new information if inserted into the 3 × 3 neighborhood [16,17].

An additional advantage is the different spatial resolution, if we should want to perform multi-resolution analysis.
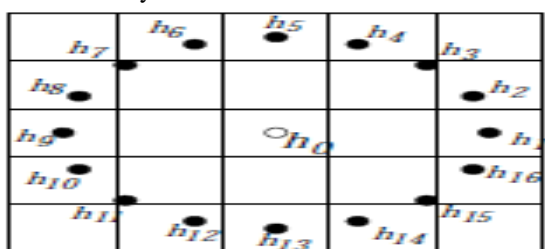
Figure 2.5: The circularly symmetric neighbor set of 16 pixels in a 5x5 neighborhood

Following the derivation of LBP_8, we first define the 16-bit version of the rotation variant LBP in Fig. 2.5.

$$LBP_{16} = \sum_{i=1}^{16} s(hi - h0)2^{i-1} \qquad (10)$$

The LBP_{16} operator has 65536 (2^{16}) different output values and 243 different rotation invariant patterns can occur in the circularly symmetric set of 16 pixels. Choosing again the uniform rotation invariant patterns that have at most two 0/1 transitions, we define LBP_{16}^{riu2}, the 16-bit version of LBP_8^{riu2}:

$$LBP_{16}^{riu2} = \{\sum_{i=1}^{16} s(hi - h0)2^{i-1} \qquad if\ U(\text{LBP16}) \leq 2\ or\ 17\ otherwise \qquad (11)$$

Thus, the LBP_{16}^{riu2} operator has 18 distinct output values, of which values from 0 (pattern 00000000000000002) to 16 (pattern 11111111111111112) correspond to the number of 1 bits in the 17 unique uniform rotation invariant patterns, and value 17 denotes the miscellaneous class of all non-uniform patterns. In practice the mapping from LBP_{16} to LBP_{16}^{riu2} is implemented with a lookup table of 216 elements [18-20].

¬ **LBP Results:**

Implementing above mentioned LBP (operators) technique for feature extraction we get following output and satisfactory results are found with good success rate. We carried out our experiment for the X-ray images from IRMA database, on near about 300 hand and spine images
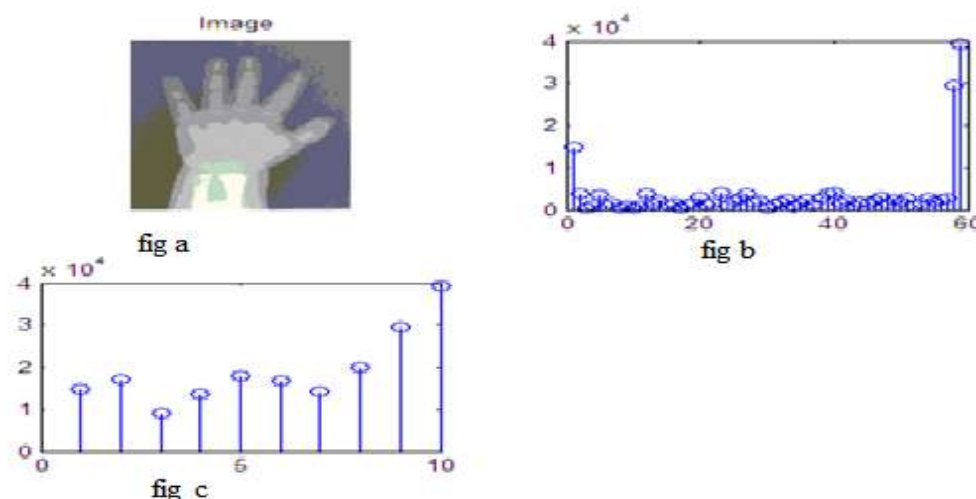
Figure 2.6: LBP results: a- Original Hand Image, b-Uniform Rotation Invariant Pattern Histogram , c-Uniform Pattern Histogram

In the case of LBP_8^{riu2} nine 'uniform' patterns out of the 36 possible patterns are chosen, merging the remaining 27 under the 'miscellaneous' label. Similarly, in the case of LBP_{16}^{riu2} consider only 7% (17 out of 243) of the possible rotation invariant patterns. Taking into account a minority of the possible patterns, and merging a majority of them, could imply that most of the pattern information is been not considered. However, this is not the case, as the 'uniform' patterns tend to be the dominant structure.

2.3: Implementation of HOG- Histograms of Oriented Gradients

Histograms of Oriented Gradients (HOG) are one of the well known features for object recognition HOG features are calculated by taking orientation histograms of edge intensity in a local region. Local object appearance and shape can often be characterized rather well by the distribution of local intensity gradients or edge detection.HOG features are used in the SIFT descriptor proposed by Lowe [21-23]. Initially, edge gradients and orientations are calculated at each pixel in the local region considered of an image. Then Sobel filters are used to obtain the edge gradients and orientations [24, 25]. The gradient magnitude *m(x, y)* and orientation *θ(x, y)* are calculated using the *x*-and *y*-directional as gradients *dx* (*x, y*) and *dy* (*x, y*) computed by Sobel filter as:

$$m(x, y) = \sqrt{dx(x,y)^2 + dy(x,y)^2}$$
$$\theta = \tan^{-1} dy(x,y)/dx(x,y)$$

This local region is divided into small spatial area called "cell" as shown below in figure 2.7. The size of the cell is 4 × 4 pixels. Histograms of edge gradients with 8 orientations are calculated from each of the local cells. Then the total number of HOG features becomes 128 = 8× (4×4) and they constitute a HOG feature vector. To avoid sudden changes in the descriptor with small changes in the position of the window, and to give less emphasis to gradients that are far from the center of the descriptor, a Gaussian weighting function with *σ* equal to one half the width of the descriptor window is used to assign a weight to the magnitude of each pixel [26-31].

Image gradients   Orientation Histogram
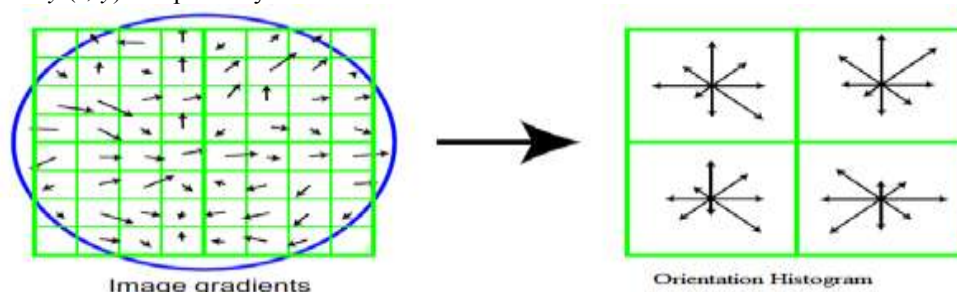
Figure 2.7: Extraction Process of HOG features. The HOG features are extracted from local regions with 16 × 16 pixels. Histograms of edge gradients with 8 orientations are calculated from each of 4 × 4 local cells. The edge gradients and orientations are obtained by applying Sobel filters. Thus the total number of HOG features becomes 128 = 8 × (4 × 4) [28].

Below Figure2.8 shows the result of HOG experiment tested on X-ray hand Image from IRMA dataset.

Figure(a)   Figure(b)   Figure(c)   Figure (d)
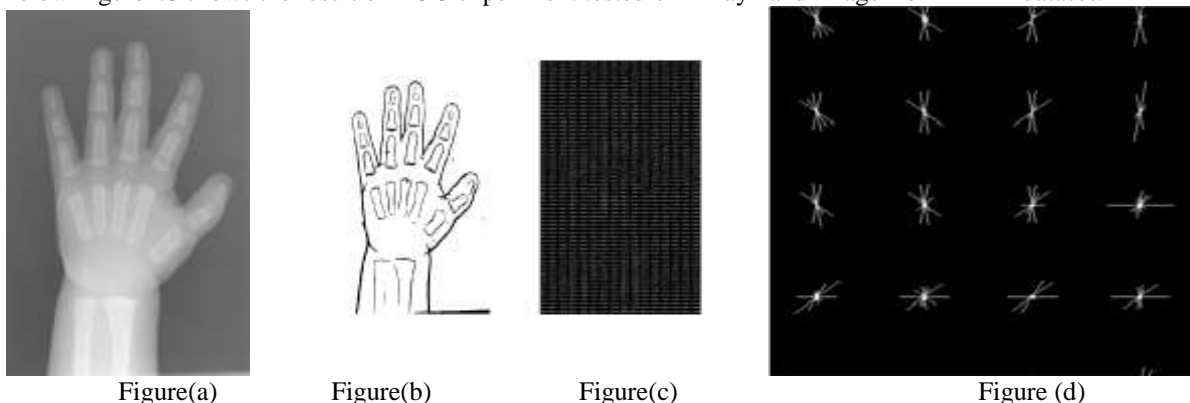
Figure 2.8: Result of HOG Experiment

The figure 2.8 from left shows(a) original x-ray hand image (3805 ×12 pixels), then (b)segmented x-ray hand image (512×512 pixels), (c)HOG Output image(1366× 662 pixels) after Extraction process which gives HOG feature size – 1× 142884 and its orientation histogram view in (d).

III. CONCLUSION

In this paper, a theoretically and computationally simple approach which is robust in terms of gray scale variations and which is shown to discriminate a large range of rotated textures efficiently is discussed. The results of Texture feature extraction methods mainly GLCM, LBP and HOG which gave us a combination of some global and local features are presented. Two rotation invariant LBP operators (LBP_8^{riu2} & LBP_{16}^{riu2}) having different spatial configuration of the circularly symmetric neighbor set, which determines the angular resolution is applied. As expected, LBP_{16}^{riu2} with its more precise quantization of the angular space provides a solid

performance. Even larger circularly symmetric neighbor sets, say 24 or 32 pixels with a suitable spatial predicate, which would offer even better angular resolution can be applied.

Also HOG features are extracted from all locations of a grid on the image as candidates of the feature vectors and can be used for classification. It is known that HOG features are robust to the local geometric and photometric transformations. If the translations or rotations of the object are much smaller than the local spatial bin size, their effect is small. In future more feature extraction process which considers another important properties like scale invariance etc., helpful for X-ray image analysis and classification can be studied.

REFERENCES

[1.]   Mohammad Reza Zare, Woo Chaw Seng, Ahmed Mueen, "Automatic Classification of Medical X-ray Images", *Malaysian Journal of Computational of Computer Science,* Vol.26 (1), 2013.
[2.]   R. M. Haralick, "Statistical and structural approaches to texture", *Proc. IEEE*, pp. 786-804, May 1979.
[3.]   T. Ojala, K. Valkealahti, E. Oja, and M. PietikaÈinen, "Texture Discrimination with Multi-Dimensional Distributions of Signed Gray Level Differences", *Pattern Recognition*, Vol. 34, pp.727-739, 2001.
[4.]   Chen, Kundu, "A Rotation and Gray Scale Transform Invariant Texture Identification Using Wavelet Decomposition and Hidden Markov Model", *IEEE Trans. Pattern Analysis and Machine Intelligence,* Vol. 16 pp.208-214, 1994.
[5.]   Wu and Wei, "Rotation and Gray-Scale Transform- Invariant Texture Classification Using Spiral Resampling, Subband Decomposition and Hidden Markov Model", *IEEE Trans. Image Processing*, Vol. 5, pp.1423-1424, 1996.
[6.]   Mikolajczyk, K., Schmid, "A performance evaluation of local descriptors", In: *Proc. of Computer Vision and Pattern Recognition* (2003).
[7.]   Dalal. N, Triggs. B., "Histograms of Oriented Gradients for Human Detection", In: *IEEE Conference on Computer Vision and Pattern Recognition* (CVPR) (2005).
[8.]   Ke, Y., Sukthankar, "R: PCA-SIFT: A more distinctive representation for local image descriptors", *In: Proc. of Computer Vision and Pattern Recognition, Washington,* pp. 66–75 (2004).
[9.]   C. M. Zhy et al., "Segmentation of Ultrasound Image Based on Texture Feature and Graph Cut", *International Conference on the Computer Science and Software Engineering*, 2008.
[10.]   R.M. Haralick et al., "Textural features for image classification", *IEEE Transaction on System*, Vol. 3, pp.610-621, 1973.
[11.]   Alaa ELEYAN1, Hasan DEM˙IREL2, "Co-occurrence matrix and its statistical features as a new approach for face recognition", Turk *J Elec Eng & Comp Science,* Vol.19, 2011.
[12.]   T. Guang Jian et al., "Automatic medical image categorization and annotation using LBP and MPEG-7 edge histograms", *International Conference on Information Technology and Applications in Biomedicine*, 2008.
[13.]   T. Deselaers et al., "Deformations, patches, and discriminative models for automatic annotation of medical radiographs", *Pattern Recognition Letters*, Vol. 29, No. 15, pp.2003-2010, 2008.
[14.]   M. PietikaÈinen, Ojala, and Z. Xu, "Rotation-Invariant Texture Classification Using Feature Distributions", *Pattern recognition*, Vol. 33, pp.43-52, 2000.
[15.]   T. Ojala et al., "A Comparative Study of Texture Measures with Classification Based on feature Distributions", *Pattern Recognition Journal*, Vol. 29, pp.51-59, 1996.
[16.]   R. Obula Konda Reddy, Dr. B. Eswara Reddy, Dr. E. Keshava Reddy, "An Effective GLCM and Binary Pattern Schemes Based Classification for Rotation Invariant Fabric Textures", *International Journal of Computer Engineering Science (IJCES),* Volume 4 Issue 1 (January 2014) ISSN: 2250:3439.
[17.]   M. Porat and Y. Zeevi, "Localized Texture Processing in Vision: Analysis and Synthesis in the Gaborian Space", *IEEE Trans. Biomedical Eng.*, Vol. 36, pp.115-129, 1989.
[18.]   R. Porter and N. Canagarajah, "Robust Rotation-Invariant Texture Classification: Wavelet, Gabor Filter and GMRF Based Schemes", *IEEE Proc. Vision, Image, and Signal Processing*, Vol. 144, pp.180-188, 1997.
[19.]   T. Randen and J.H. Husoy, "Filtering for Texture Classification: A Comparative Study", *IEEE Trans. Pattern Analysis and Machine Intelligence,* Vol. 21, pp.291-310, 1999.
[20.]   H. Tamura, S. Mori, and T. Yamawaki, "Textural Features Corresponding to Visual Perception", *IEEE Trans. Systems, Man, and Cybernetics,* Vol. 8, pp.460-473, 1978.

[21.] D. Lowe, "Object recognition from local scale-invariant features", *International Conference on Computer Vision*, pp.1150-1157, 1999.

[22.] Y. Wu and Y. Yoshida, "An Efficient Method for Rotation and Scaling Invariant Texture Classification", *Proc. IEEE Int'l Conf. Acoustics, Speech, and Signal Processing*, Vol. 4, pp.2519-2522, 1995.

[23.] D. Lowe, "Distinctive image features from scale invariant key points", *International Conference on Computer Vision,* Vol. 60, No. 2, pp.91-110, 2004.

[24.] Sobel, "An Isotropic 3×3 Gradient Operators, Machine Vision for Three – Dimensional Scenes, Freeman, H.", *Academic Pres, NY*, 1990.

[25.] Prewitt, "Object Enhancement and Extraction, Picture Processing and Psychopictorics" (B. Lipkin and A. Rosenfeld, Ed.), *NY, Academic Pres*, pp.263-269, 1970.

[26.] Roberts, L. G., Machine Perception of Three-Dimensional Solids, in optical and Electro-Optical Information Processing (J. Tippett, Ed.), MIT Press , pp.159-177, 1965.

[27.] Ziou, D. and Tabbone, S., Edge Detection Techniques - An Overview, Technical Report, No. 195, Dept. Math & Informatique, Universit de Sherbrooke, 1997.

[28.] W. T. Freeman and M. Roth, "Orientation histograms for hand gesture recognition. *Intl. Workshop on Automatic Face and Gesture- Recognition", IEEE Computer Society, Zurich, Switzerland*, pp.296-301, June 1995.

[29.] W. T. Freeman, K. Tanaka, J. Ohta, and K. Kyuma, "Computer vision for computer games", *2nd International Conference on Automatic Face and Gesture Recognition, Killington, VT, USA*, pp.100-105, October 1996.

[30.] D. M. Gavrila, "The visual analysis of human movement: A survey", *CVIU*, 73(1), 1999.

[31.] L.Wang and G. Healey, "Using Zernike Moments for the Illumination and Geometry Invariant Classification of Multi-Spectral Texture", *IEEE Trans. Image Processing*, Vol. 7, pp.196-203, 1998.